Optimization of the Electronic Third-order Nonlinearity of Cyanine-like Molecules for All Optical Switching

Honghua Hu[1], Trenton R. Ensley[1], Matthew Reichert[1], Manuel R. Ferdinandus[1,6], Davorin Peceli[1], Olga V. Przhonska[1,2], Seth R. Marder[4], Alex K.-Y. Jen[5], Joel M. Hales[4], Joseph W. Perry[4], David J. Hagan[1,3], and Eric W. Van Stryland[1,3]

[1]CREOL: College of Optics & Photonics, University of Central Florida, Orlando, FL 32816, USA; [2]National Academy of Sciences Kiev, Ukraine; [3]Department of Physics, University of Central Florida, Orlando, FL 32816, USA; [4]School of Chemistry and Biochemistry and Center for Organic Photonics and Electronics, Georgia Institute of Technology, Atlanta, GA 30332, USA; [5]Department of Materials Science & Engineering, University of Washington, Seattle, WA 98195, USA; [6]Department of Engineering Physics, Air Force Institute of Technology, Dayton, OH 45433

Contact e-mail: ewvs@creol.ucf.edu

ABSTRACT

All optical switching (AOS) applications require materials with a large nonlinear refractive index (n_2) but relatively small linear and nonlinear absorption loss. The figure-of-merit (FOM), defined as the ratio between the real and imaginary parts of the second hyperpolarizability (γ), is widely used to evaluate the operating efficiency of AOS materials. By using an essential-state model, we describe the general dispersion behavior of γ of symmetric organic molecules and predict that the optimized wavelength range for a large FOM is near its linear absorption edge for cyanine-like dyes. Experimental studies are normally performed on organic solutes in solution which becomes problematic when the solvent nonlinearity dominates the total signal. This has been overcome using a Dual-arm Z-scan methodology to measure the solution and solvent simultaneously on two identical Z-scan arms and discriminating their small nonlinear signal difference. This technique significantly reduces the measurement uncertainty by correlating the excitation noise in both arms, leading to nearly an order-of-magnitude increase in sensitivity. Here we investigate the n_2 and two-photon absorption (2PA) spectra of several classes of cyanine-like organic molecules and find that the results for most molecules agree qualitatively and quantitatively with the essential-state model. Many cyanine-like molecules show a relatively small FOM due to the presence of large 2PA bands near the linear absorption edge; however, an exception is found for a thiopyrylium polymethine molecule of which the maximum FOM can be > 400, making it an excellent candidate for AOS.

Keywords: All optical switching; Nonlinear optics, spectroscopy; quantum perturbation theory.

1. INTRODUCTION

The development of organic cyanine-like molecules for optimized third-order nonlinearity has gained significant traction in the research community due to their potential application for all-optical switching (AOS) applications [1]. Efficient AOS devices require materials with large nonlinear refraction (NLR), characterized by the nonlinear refractive index n_2, and small optical losses. Typically, the dominant loss mechanism in the spectral regions of interest is two-photon absorption (2PA), which is characterized by the 2PA coefficient α_2. The n_2 and α_2 are related to the real and imaginary parts of the second hyperpolarizability γ, respectively, and depend not only on the nonlinearity per molecule of the dye itself, but also that of the solvent, the dye concentration, and local field effects as shown below:

$$\mathrm{Re}\,\gamma^{(3)} \propto \frac{n_2 n_0^2}{N f^4}, \tag{1}$$

$$\mathrm{Im}\,\gamma^{(3)} \propto \frac{\alpha_2 n_0^2 \lambda_0}{N f^4}, \tag{2}$$

where n_0 is the linear refractive index of the medium in which the molecules are embedded, N is the number density of molecules, f is the local field correction defined as $(n_0^2+2)/3$, and λ_0 is the wavelength. Furthermore, we can write the molecular nonlinearity in terms of its 2PA and NLR cross sections as follows [2,3]:

$$\delta_{\text{2PA}} = \frac{\hbar\omega}{N}\alpha_2, \tag{3}$$

$$\delta_{\text{NLR}} = \frac{\hbar\omega}{N}k_0 n_2, \tag{4}$$

where $\hbar\omega$ is the incident photon energy and $k_0 = 2\pi/\lambda_0$ is the vacuum wavenumber. Here the units for the cross sections are Göppert-Mayer (GM) defined as 10^{-50} cm^4·s·molecule^{-1}·photon^{-1}. To characterize the quality of the molecule for AOS applications, a useful figure of merit is introduced [1,2].

$$\text{FOM} \equiv \left|\frac{\text{Re}(\gamma^{(3)})}{\text{Im}(\gamma^{(3)})}\right| = 2\left|\frac{\delta_{\text{NLR}}}{\delta_{\text{2PA}}}\right|. \tag{5}$$

In this work we experimentally investigate the spectra of δ_{NLR} and δ_{2PA} in a number of organic dyes experimentally using Z-scan techniques [4,5]. A variation of the so called "sum-over-states" (SOS) model is then used to fit the measured spectra to gain insight into the physical causes of the nonlinear parameters and hence the FOM. The knowledge of the physical origins will allow us to more efficiently engineer organic molecules that are better suited for AOS devices and applications.

2. ESSENTIAL-STATE MODEL AND OPTIMIZATION

The standard recipe to describe the dispersion of the bound electronic nonlinearity of organic molecules is the SOS model, which takes into account the ground state and all possible excited states and their corresponding transition dipole moments [6,7]. For a molecular system which contains an infinite number of excited states, the SOS model is computationally difficult to manage; therefore, a variation of the SOS model, named the essential-state model which contains the most important states, was developed to describe the low energy physics of organic molecular nonlinearities [8]. For centrosymmetric molecules possessing zero permanent dipole moment, we use an essential-state model considering only: the ground state (g) with *even* symmetry, the 1st excited state (e) with odd symmetry, and a higher-lying excited state (e') with *even* symmetry known as a 2PA final state. However, we also allow the possibility of multiple 2PA final states using the same intermediate state. This is referred to as a quasi-3-level model. The transition from the ground state g to the 1st excited state e, and from e to the 2PA final state e', are electric dipole allowed due to the selection rule (*even*→*odd*); while the direct transition between ground state and 2PA final state with the same symmetry, *even*→*even*, is forbidden. In this case, the frequency response for the second hyperpolarizability deduced from the SOS model can be drastically simplified to include only the main resonant terms:

$$\gamma(\omega) \propto \frac{\mu_{ge}^2 \mu_{ee'}^2}{\left(\overline{\Omega}_{ge} - \hbar\omega\right)^2\left(\overline{\Omega}_{ge'} - 2\hbar\omega\right)} - \frac{\mu_{ge}^4}{\left(\overline{\Omega}_{ge} - \hbar\omega\right)^3} \tag{6}$$

where $\overline{\Omega} = E - i\Gamma$ defines the transition frequency Ω and linewidth between states g and e *or* e', and μ_{ge} and $\mu_{ee'}$ are the transition dipole moments between states g and e and states e and e', respectively. In this overly simplified expression, the first term is called the "Two-photon term" (T-term), corresponding to the transition between the ground state (g) and the 2PA final state (e'). The second term, which always shows a negative contribution, is called the "Negative term" (N-term), corresponding to the transition between the ground state (g) and the intermediate state (e). This term is sometimes referred to as virtual saturation since it corresponds to real saturation near the 1-photon resonance. From Eq. (6), for centrosymmetric molecules, the overall nonlinearity is due to the competition of these two terms, and is determined by the magnitude of the transition dipole moments and the relative energies of the relevant states. Shown in Fig. 1 (a) is the dispersion of the real and imaginary parts of $\chi^{(3)}$ (= $Nf^4\gamma^{(3)}/\varepsilon_0$ where ε_0 is the electric permittivity of free space) calculated by the essential-state model for a "virtual" molecular system with three energy levels. A peak of the imaginary part of $\chi^{(3)}$, corresponding to a 2PA resonance, is observed at $\Omega_{e'g}/2$. This 2PA resonance is from the T-term. The real part of $\chi^{(3)}$, corresponding to the bound electronic NLR, initially increases gradually from a small negative value in the DC limit ($\omega \to 0$) to a positive peak slightly red-shifted from the 2PA peak. It then decreases drastically becoming negative as the incident photon energy increases beyond the 2PA peak. This n_2 spectral shape near the two-photon resonance is the

signature of the Kramers-Kronig (KK) relations [9]. As the incident photon energy approaches the absorption gap of the material, corresponding to $\omega \rightarrow \Omega_{eg}$, the N-term starts to dominate all other nonlinear contributions, and a large negative n_2 is thus observed. The FOM spectrum is shown in Fig. 1b using the specific parameters in the figure caption; a relatively small FOM plateau is observed at the low frequency side of the 2PA band ($\omega < \Omega_{eg}/2$) due to the presence of the n_2 peak near this spectral vicinity. Only when the frequency approaches the 1PA edge does the FOM dramatically increase. It is important to stay below the one-photon absorption edge to minimize optical losses. Note that as you approach the DC limit there is essentially no 2PA which inherently yields a large FOM; but with these parameters the NLR is negative and quite small [11]. This is what we observe for squaraines. For other parameters, the DC limit can give positive NLR and the second zero in the FOM on the low frequency side disappears.

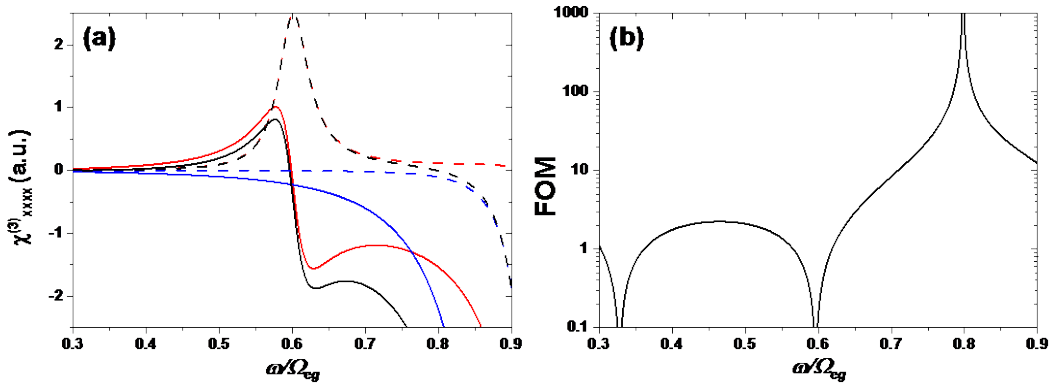

Figure 1. 3-level essential-state model calculation, Eq. (6), of the spectrum of (a) real (solid) and imaginary (dashed) parts of $\chi^{(3)}$, including T-term (red), N-Term (blue), and total (black), and (b) FOM calculated from part (a), as the function of input photon frequency normalized by Ω_{eg}. Parameters use were $\Omega_{e'g} = 1.2\Omega_{eg}$, $\Gamma_{eg}/\Omega_{eg} = 200$, $\Gamma_{e'g}=10\Gamma_{eg}$, $|\mu_{ge}|=|\mu_{e\,e'}|$.

3. EXPERIMENTAL TECHNIQUE – DUAL ARM Z-SCAN

To measure the nonlinearity of organic molecules, one of the standard techniques is the Z-scan, which simultaneously measures both the NLR and nonlinear absorption properties of the material using a single beam [4]. Typically these molecules need to be measured in solution in which two separate Z-scans are performed to extract its nonlinearity: one on the solution and the other on the neat solvent. However, for molecules with limited solubility,

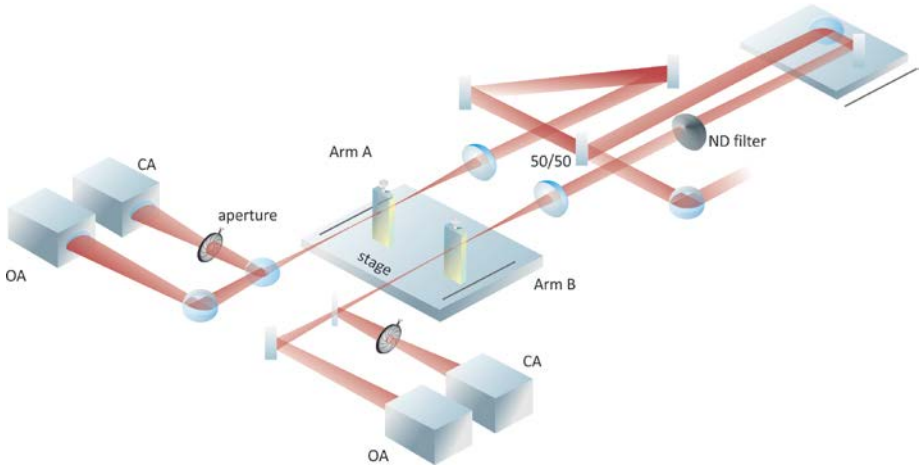

Figure 2. Dual-arm Z-scan schematic [5].

despite large molecular nonlinearity, the nonlinear signal from the organic solute can be quite small compared to the nonlinear signal background from the solvent. Thus when subtracting the solvent signal from the solution signal, the resultant solute signal can be masked by the noise of the two sequential measurements. To overcome this difficulty, we

recently developed the Dual-arm Z-scan (DA Z-scan) technique [5] which simultaneously measures both the solution and the solvent on two identical Z-scan arms as shown in Fig. 2 allowing for the real time subtraction of the two to obtain the solute signal. This requires an identical irradiance distribution in both arms, i.e. pulse energy, beam waist, and pulse width, as well as matching sample positions, sample cuvettes, and photodetectors. Simultaneous subtraction, as opposed to sequential subtraction with conventional Z-scans, allows for the correlation of the noise from the excitation source (i.e. fluctuating pulse energy, beam pointing stability, beam size, pulse width, etc.) on each arm which greatly suppresses the measurement uncertainty of the organic molecule, leading to an order of magnitude increase in measurement sensitivity. It has been shown that this technique allows for the measurement of solute n_2's nearly an order of magnitude smaller than that of the solvent, and 1.5× smaller than that of the quartz cuvettes [5]. This enhancement in sensitivity becomes particularly important when measuring at spectral regions where the NLR changes sign and while approaching the DC limit where the NLR is predicted by the essential-state model to be small. We use this technique as well as conventional Z-scans to measure the nonlinear dispersion of the organic molecules studied.

4. RESULTS AND DISCUSSION

Figure 3 shows the linear absorption and structures of a squaraine molecule named SD-O 2405 dissolved in toluene (Fig. 3a) [12], an extended quadrupolar molecule named SJZ-3-16 dissolved in tetrahydrofuran (Fig. 3b) [2,13], a thiopyrlium polymethine dye named YZ-V-69 dissolved in carbon tetrachloride (Fig. 3c), and a tricyanine molecule named AJTC-02 dissolved in dichloromethane (Fig. 3d). The spectra of NLR and 2PA were measured using the dual-arm Z-scan method for SD-O 2405 and AJTC 02, conventional Z-scans for YZ-V-69, and two-photon induced fluorescence as well as conventional and WLC Z-scans [2,4] to measure the 2PA and NLR spectra of SJZ-3-16, respectively.

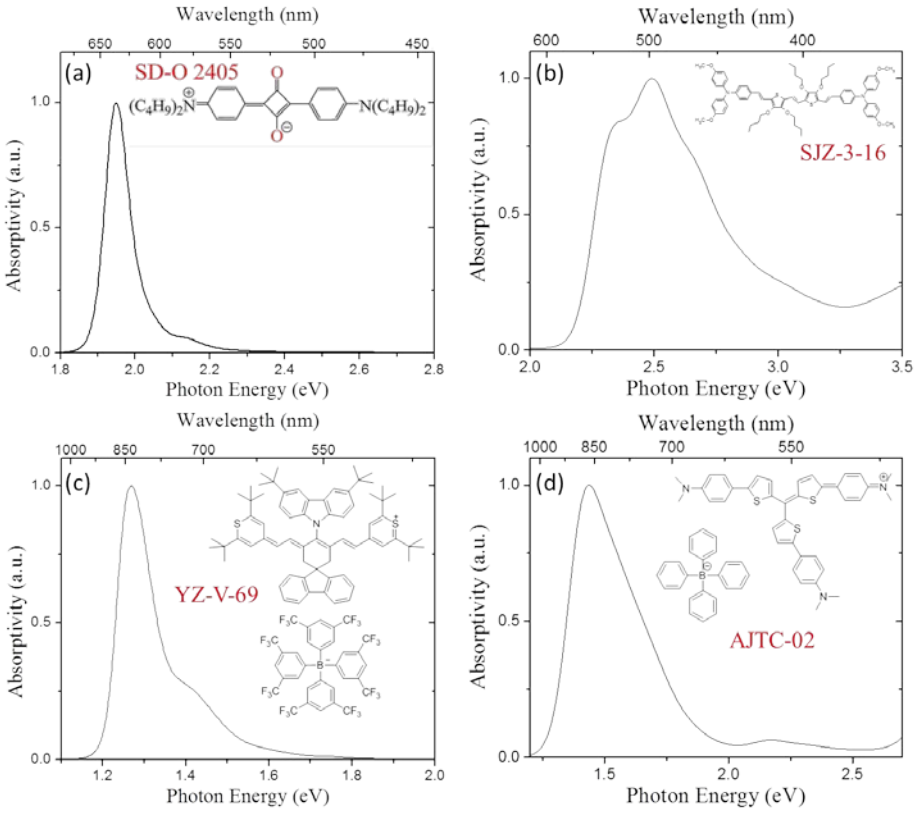

Figure 3. Linear absorption spectra and structures of (a) a squaraine molecule dissolved in toluene, (b) an extended electron-rich chromophore quadrupolar molecule dissolved in tetrahydrofuran, (c) a thiopyrlium polymethine dye dissolved in carbon tetrachloride, and a (d) tricyanine molecule dissolved in dichloromethane.

The linear absorption peak for SD-O 2405, corresponding to the transition between the ground state and 1st excited state, is located at 1.95 eV (636 nm). Two 2PA bands are observed at 1.48 eV and 1.77 eV corresponding to 2PA final

states at 2.95 eV and 3.54 eV, respectively. These two 2PA states are associated with the S_2 and S_4 (i.e. different *e'* final states) electronic states of the molecule, as verified by quantum chemical calculations [12]. Assuming these 2PA transitions share the same intermediate 1PA state (i.e. *e*), the essential-state model is expanded to account for multiple 2PA final states to fit the 2PA spectrum. The calculated spectra from the essential-states model agree well with the experimental results. All n_2 values were experimentally found to be negative due to the large value of μ_{ge} compared to $\mu_{ee'}$ (e.g., $e' = S_2$) and compared to that of a relatively higher lying 2PA final state (e.g., S_4). A relatively large magnitude of n_2 is measured close to the linear absorption edge at 1.8 eV yielding δ_{NLR} = -32000 GM originating from the enhanced N-term as discussed in section 2. However, due to the presence of a 2PA band near the 1PA edge, the FOM, is found to be less than 5.

The essential-state model can also be used to fit the 2PA spectrum and n_2 dispersion of an extended quadrupolar molecule, SJZ-3-16. The first 2PA band is observed at 800 nm (corresponding to the 2PA final state at 3.1 eV) with peak δ_{2PA} of 500 GM, and the second at 650 nm (2PA final state at 3.8 eV) with peak δ_{2PA} of 3,900 GM. More interesting is the δ_{NLR} dispersion; a positive δ_{NLR} ~120 GM is observed at 710 nm, which then increases to 730 GM at 690 nm. However, δ_{NLR} changes sign from positive to -410 GM at 670 nm, followed by a dramatic increase of its *negative* magnitude as the photon energy approaches the linear absorption edge. Note that δ_{NLR} cannot be resolved at photon energies below 1.7 eV (wavelength > 730 nm) due to indistinguishable signals between the solution and solvent measured by conventional Z-scans. Both the spectrum of δ_{2PA} and dispersion of δ_{NLR} can be fit by the essential-state model with two 2PA final states. The small variation of δ_{NLR} fitting at ~800 nm, originating from the first weak 2PA band (3.1 eV), is difficult to verify due to its small magnitude. The positive δ_{NLR} peak at 690 nm, originating from the transition into the second 2PA band (3.8 eV), can be fit with an excited state transition dipole moment $\mu_{ee'}$ ~25% larger than μ_{ge}. Therefore, the positive δ_{NLR} peak is the result from 1) the large magnitude of $\mu_{ee'}$ and 2) the photon energy of this 2PA state being far below the 1PA peak. Similar to SD-O 2405, the FOM is small (less than 3), due to the presence of a strong nearby 2PA band.

Due to YZ-V-69's relatively large solubility, which allows for concentrations greater than 10^{-3} M, and large δ_{NLR}, conventional Z-scans were sufficient to distinguish the nonlinear signal of the solute in the solution from that of the pure solvent. Interestingly for this molecule only one 2PA band is observed located at the vibrational shoulder of its main 1PA transition ($g \rightarrow e$) (λ ~ 1700 nm), but no 2PA or ESA is observed near its linear absorption edge. On the other hand, the δ_{NLR} of the molecule is negative at all wavelengths of measurement, and its magnitude increases dramatically near the linear absorption edge. As a result, the FOM is quite large, being > 400 near the absorption edge, 42 at 1300 nm, and 10 at 1550 nm, making this dye an excellent candidate material for AOS. This is despite the fact that there is a 2PA allowed (1PA forbidden) transition at 1200 nm, as suggested by fluorescence anisotropy measurements. The essential-state model fitting indicates an extremely small $\mu_{ee'}$, leading to a negligible contribution from the T-terms from this 2PA final state. Hence the dispersion of δ_{NLR} is completely dominated by the N-terms. The 2PA fitting by the essential-state

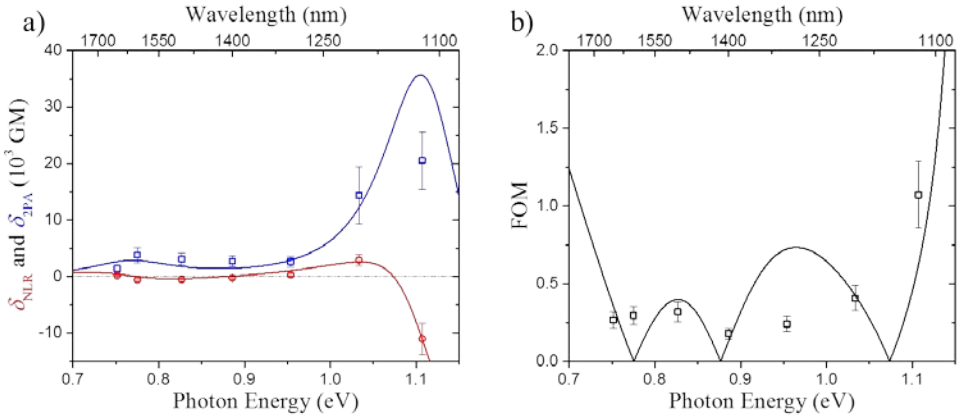

Figure 4. (a) 2PA and NLR cross sections for AJTC-02 with essential-state model fits and (b) FOM from experimentation and essential-state fits.

model exhibits a negative value of δ_{2PA}. This "negative 2PA" appears as an unphysical prediction of the 3-level essential state model, and means to correct for this need to be investigated further.

The essential-state model can also be used to describe molecules that do not possess centrosymmetry in their molecular structure, although the model now needs to include the change in permanent dipole moments between ground and excited states, i.e. the so-called dipole, D, term [7]. Shown in Fig. 4a is the spectrum of 2PA and dispersion of NLR of the tricyanine molecule AJTC-02 dissolved in dichloromethane (DCM) measured by DA-Z-scan. The 2PA spectrum shows two 2PA bands at 1600 nm and 1100 nm with δ_{2PA} of 3800 GM and 20550 GM respectively. Using fitting parameters obtained from the 2PA spectrum, the n_2 dispersion can be fit reasonably well with the essential-state model. Note that the sign of δ_{NLR} changes twice at 1550 nm and 1400 nm. This is an indication of the competition between T-terms and N-terms of similar magnitude, leading to even smaller FOM, as shown in Fig. 4b. Therefore, to increase the FOM, the key challenge is to suppress the nonlinear absorption in the spectral range where n_2 is still large. Since the large positive n_2 arising from T-terms is always paired with a 2PA transition, it is unrealistic to have a large FOM. Therefore, the optimized approach to increase the FOM is to take advantage of the resonant N-terms near the 1PA edge to enhance n_2 and suppress nonlinear absorption. However, the challenge is to obtain a large FOM before the tail of the 1PA becomes too large. Note that not only 2PA but also other nonlinear absorption mechanism, such as ESA, may contribute to the optical losses in this spectral region.

CONCLUSIONS

We have experimentally determined the third-order nonlinear refraction (NLR) dispersion and two-photon absorption (2PA) spectrum of several classes of organic dyes by utilizing conventional and Dual-arm Z-scan techniques and fit their spectra with an essential-state model. Excellent quantitative and qualitative agreement was shown to exist for such a simplification to the sum-over-states model except near the linear absorption edge where the 3-level model predicts negative 2PA. It is observed that the greatest opportunity to obtain a large FOM lies just outside the one-photon absorption edge but before any 2PA resonance where the nonlinear and linear optical losses are at a minimum. We can, thus, apply the essential-state model with knowledge of the physical nonlinear parameters to improve the design and development of future organic molecules for nonlinear optical applications.

Acknowledgements: This material is based upon work supported by the National Science Foundation under Grants, ECS#1202471, MRI 1229563, and AFOSR MURI grant FA9550-10-1-0558.

REFERENCES

[1]. J. M. Hales *et al.*, *Science*, **327**, 1485-1488 (2010).
[2]. M. Balu *et al.*, *J. Opt. Soc. Am. B*, **25**, 159-165 (2008).
[3]. M. Göppert-Mayer, *Ann. Phys.*, **401**, 273-294 (1931).
[4]. M. Sheik-Bahae *et al.*, *IEEE J. Quantum. Elect.*, **26**, 760-769 (1990).
[5]. M. R. Ferdinandus *et al.*, *Opt. Mater. Express*, **2**, 1776-1790 (2012).
[6]. J. F. Ward, *Rev. Mod. Phys.*, **37**, 1-18 (1965).
[7]. B. J. Orr *et al.*, *Mol. Phys.*, **20**, 513-526 (1971).
[8]. M. G. Kuzyk *et al.*, *Phys. Rev. A*, **41**, 5098-5109 (1990).
[9]. D. C. Hutchings *et al.*, *Opt. Quant. Electron.*, **24**, 1-30 (1992).
[10]. E. Zojer *et al.*, *Chem. Eur. J.*, **10**, 2668-2680 (2004).
[11]. G. I. Stegeman *et al.*, *Nonlinear Optics: Phenomena, Materials and Devices*; John Wiley & Sons, Inc: Hoboken, NJ, (2012)
[12] S. Webster *et al.*, J. Phys. Chem. Lett. **1**, 2354-2360 (2010).
[13] S. Zheng *et al.*, Chem. Commun. (Cambridge) **13**, 1372-1374 (2007).